

MICROSTRUCTURE BASED FLOW CURVE MODELING OF HIGH-MN STEELS WITH TWIP AND TRIP EFFECT

RAPHAEL TWARDOWSKI*, ULRICH PRAHL

IEHK RWTH Aachen, Intzestrasse 1, 52071 Aachen

**Corresponding author: raphael.twardowski@iehk.rwth-aachen.de*

Abstract

In the present work a microstructural model based on representative volume elements (RVE) is proposed for high manganese steels with TWIP and TRIP effect. The polycrystalline structure is generated by spatial discretization of the RVE in three-dimensional Voronoi tessellations. For the hardening behavior a constitutive material model is used based on the evolution of dislocation, twin and epsilon-martensite density. The plastic deformation is investigated numerically using periodic displacement boundary conditions. In addition to the parameters of temperature and microstructure the influence of the chemical heterogeneity is investigated. The experimental verification of the numerical results is done by uniaxial tensile tests on flat tensile specimens.

Key words: high manganese steels, microstructure, representative volume element, twinning, phase transformation

1. INTRODUCTION

High manganese steels exhibit their excellent mechanical properties due to the different deformation mechanisms such as the martensitic transformation and mechanical twinning. As already reported by Allain et al. (2004a), Bouaziz et al. (2008), twin boundaries act as strong obstacles to dislocation movement. By increasing the twin volume fraction the dynamic Hall-Petch effect leads to an additional hardening effect by reducing the mean free path. The activation of the dominating deformation mechanism is mainly dependent on the current stacking fault energy (SFE) according to Allain et al. (2004b), Lee and Choi (2000). In the present work a microstructural model based on representative volume elements is proposed for high manganese steels with TWinning Induced Plasticity (TWIP) and TRAnsformation Induced Plasticity (TRIP) effect. The polycrystalline structure is generated by spatial discretization of the Representative Volume Element

(RVE) in three-dimensional Voronoi tessellations. On this polycrystalline scale Melchior (2009) presented results on the deformation behavior of high manganese steels using Crystal Plasticity Finite-Element Method (CPFEM) routine. In this work a constitutive material model is used based on the evolution of dislocation and twin density for describing the hardening behavior. The plastic deformation is investigated numerically using periodic displacement boundary conditions. In addition to the effect of temperature, the influence of the microstructure is investigated. The experimental validation of the numerical results is done by uniaxial tensile tests on flat tensile specimens. Twin and martensite volume fraction is investigated by Electron Back Scatter Diffraction (EBSD) experiments on the fractured tensile specimens for verification of the calculated total phase fractions.

2. EXPERIMENTAL PROCEDURE

In order to determine the influence of temperature on a specific alloy, the testing material was chosen based on the mechanism map, which was developed in a previous work by Saeed-Akbari et al. (2009). By adjusting the stacking fault energy the different deformation mechanism can be investigated in isolated and in mixed mode by only changing the temperature. The material is available as hot rolled sheet with a composition according to table 1. In order to investigate the influence of different grain sizes, the initial microstructure was modified by annealing at different temperatures. The initial material with an average grain size of 2 μm was annealed at 1070 K, 1170 K and 1300 K for 30 min and subsequently water quenched. Then the sheets were machined into tensile samples by water jet cutting and pre-strained to 5 %, 10 %, 20 %, 30% and 40 %, in order to reveal the evolution of the phase transformation mechanisms. The tensile tests were carried out for a temperature range of 123 K to 423 K and a strain rate of 0,004 1/s. The characterization was realized by light optical microscopy (LOM), X-ray diffraction (XRD) and EBSD.

Table 1. Chemical composition of the investigated high-Mn steel.

Fe	C	Mn	Si	Cr	Ni	Al	N	Nb	V
Bal.	0.58	22.48	0.025	0.074	0.030	0.004	0.009	0.019	0.219

3. REPRESENTATIVE VOLUME ELEMENT

The modeling of the metal microstructure at grain scale within this work was carried out by representative volume elements (RVE). Efficient tools for Voronoi tessellation and meshing, as developed in Rycroft (2009) and Geuzaine and Remacle (2009) already exist. The common drawback is the lack of conversion options into specific formats. The polycrystalline volume structure in this work is generated by mesh based volume discretization. For the creation of this structure a Voronoi cell generator was developed, which is able to create a polycrystalline volume model. In order to guarantee a representative volume, the model is geometrically periodic in each spatial direction. The mesh is established by cubic elements and the grain structure is generated by means of raster space discretization. All elements are arranged by the nearest neighbor sweep circle method, which aligns all elements within an incrementally growing circle to a specific seed point within the RVE. Another method is to calculate the

minimum distance between an element and all seeds, which is more accurate but because of the explicit calculation method not efficient for large element numbers. The numerical tensile test on micro-scale requires appropriately chosen boundary conditions for homogenization, which are considering the physical processes in the boundary region. Sufficient results were achieved with periodic boundary conditions, which were implemented according to Kassem (2009). The boundary conditions consist of a set of prescribed displacements and linear constraints between nodes on the RVE boundaries. The resulting RVEs simulate the periodicity conditions on the microstructure and result in periodic deformations and anti-periodic tractions on the boundaries of the RVE. The usual approach for homogenization is to compare a constitutive relation between averages, relating volume averaged field variables. Consequently, the so called effective properties can be used in macroscopic analysis. The simulations give the homogenized stress response in terms of the first Piola-Kirchhoff stress tensor \mathbf{P} , that results from a prescribed macroscopic deformation gradient tensor \mathbf{F} .

4. MATERIAL MODEL

Deformation twinning and phase transformation can occur in mixed and single mode, which highly depends on the local stacking fault energy. The critical SFE is chosen to be 20 mJm^{-2} (Frommeyer et al. 2003; Saeed-Akbari et al., 2011; Dumay et al., 2008; Jin & Lee, 2009). The description of the plastic deformation by a polycrystalline volume element requires the consideration of different material models for each deformation mechanism. The material model is based on the Taylor approach for describing the hardening behavior and the Kocks-Mecking method for calculation of the dislocation density (Kocks & Mecking, 2003). The link to the additional hardening effect caused by the TWIP effect is established by considering a stress induced twin density as considered by Bouaziz et al. (2008) and Allain et al. (2004c). The phase transformation from austenite to ϵ -martensite, is described by a modified Olsen-Cohen model (Olson & Cohen, 1974). The model is implemented as UHARD subroutine in the Abaqus Finite Element software environment.



4.1. Austenite phase

The macroscopic stress σ of the austenitic phase can be calculated by the relation between the statistically stored dislocation density ρ and the flow stress σ as follows:

$$\sigma = \sigma_0 + \alpha M G b \sqrt{\rho} \quad (1)$$

Following the assumption of the Kocks-Mecking theory, the evolution of the dislocation density with deformation is the result of the competition between the rate of production and the annihilation rate of dislocations, according to:

$$\frac{d\rho}{d\varepsilon} = M \left(\frac{1}{bd} + \frac{k}{b} \sqrt{\rho} - f\rho \right) \quad (2)$$

In those equations, ρ_γ is the dislocation density, b is the burgers vector, λ is the mean free path for dislocations, G is the shear modulus, α is a numerical factor that characterizes the dislocation - dislocation interaction, k and f are fitting parameters. d is assumed to be equal to the grain size for the austenite phase. The yield strength σ_0 [MPa] is dependent on the chemical composition.

$$\sigma_0 = 128 + 187C + 2Mn \quad (3)$$

With C, Si and Cr content in wt. %. The reduction of the grain size d by increasing twin and ε -martensite volume fraction is calculated by:

$$d = d_{init} \sqrt[3]{1-F} \quad (4)$$

with d_{init} the initial grain size, F the phase volume fraction of twins and ε -martensite.

4.2. TWIP

The TWIP effect is assumed as strain induced plastic deformation. The evolution of the twin density is usually described by an empirical law (Eq. 6). Assuming a critical twinning stress the onset of deformation twinning is calculated for each grain. In this work the critical twinning stress σ_c is used, which has to be overcome in order to initiate twinning according to Gutierrez-Urrutia et al. (2010).

$$\sigma_c = M \frac{\gamma_{sfe}}{b} - \frac{K_{HP}}{\sqrt{d}} \quad (5)$$

Where γ_{sfe} is the stacking fault energy calculated as described in Saeed-Akbari et al. (2009) and K_{HP} the Hall-Petch constant. The critical twinning stress is highly dependent on the stacking fault energy, the

grain size and the orientation of the grain. The twin volume fraction F_{twin} is calculated by the following equation, which was already used in Choi et al. (1999):

$$F_{twin} = \left(1 - \exp(-B_{twin} \varepsilon^n) \right) F_{twin}^{sat} \quad (6)$$

B_{twin} is related to the nucleation rate of twins and is dependent on the stacking fault energy and $n = 1.4$ is a fitting parameter. F_{twin}^{sat} is the twinning saturation volume fraction, which is also controlled by the stacking fault energy. The hardening effect is accounted by the reduction of the grain size according to (4). The additional dislocation evolution and influence on the dislocation density is calculated by extending equation 2 to:

$$e_{min} \frac{2d_{111} \gamma}{Gb} d, \quad (7)$$

Here e is the minimum twin thickness, which is calculated according to:

$$e_{min} \frac{2d_{111} \gamma}{Gb} d, \quad (8)$$

where b is the Burgers vector and d_{111} the distance between the 111 planes.

4.3. TRIP

The ε -martensite volume fraction F_ε is calculated by the modified Olson-Cohen law Olson and Cohen (1974):

$$F_\varepsilon = \left(1 - \exp(-B_\varepsilon \varepsilon^n) \right) F_\varepsilon^{sat} \quad (9)$$

B_ε is related to the volume of shear bands, F_ε^{sat} is the twinning saturation volume fraction and $n = 1.0$ is a fitting parameter. The calculated ε -martensite volume fraction changes the resulting total stress of the ε -martensite/austenite constituent.

$$\sigma_\varepsilon = \sigma_{\varepsilon 0} + \alpha G \sqrt{b} \sqrt{\frac{1 - \exp(-Mf\varepsilon)}{fL_0}} \quad (10)$$

In this equation $\sigma_{\varepsilon 0}$ is the yield stress for the martensitic phase, f is a fitting parameter and L_0 the mean ε -martensite lath width. The total stress is calculated by a mixture law, as proposed by Bouquerel et al. (2006):

$$\sigma = \sigma_\gamma (1 - F_\varepsilon^n) + \sigma_\varepsilon F_\varepsilon^n \quad (11)$$



where $n = 2$ is a fitting parameter, σ_γ the austenite and σ_ε respectively the martensite stress. All model parameters are summarized in table 2.

Table 2. Summary of relevant model parameters.

Parameter	Value	Source
α	0.3628 [-]	Bouquerel et al. (2006)
G	65 GPa	Allain et al. (2004a)
b	$2.5 \cdot 10^{-10}$ m	Allain et al. (2004a)
k	0.015 [-]	Allain et al. (2004c)
f	1.5 [-]	
K_{HP}	356000 MPa/ μm	Gutierrez-Urrutia et al. (2010)
d_{111}	$6.68 \cdot 10^{-10}$ m	Allain et al. (2004c)
L_0	0.2 μm	Bouquerel et al. (2006)

creased temperatures whereas ε -martensite formation is dominant at low temperatures (figure 2).

This observation is accordant to the results made by Saeed- Akbari et al. (2012). Assuming a constant temperature for the entire sample, the appearance of both deformation mechanism at 293 K can be explained by microsegregation and different grain size. Segregations of manganese and carbon are influencing the SFE directly. In figure 3 the mechanical properties are summarized. With increasing temperature and grain size the tensile and yield strength are lowered. On the contrary the failure strain is improved by a more coarse microstructure and higher temperature. Alongside figure 3 indicates the transition area, where both mechanisms are observed. Four to five layers of stacking faults are re-

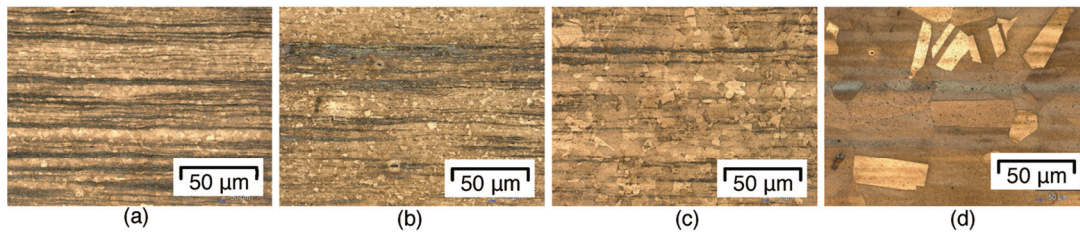


Fig. 1. Light optical micrographs of initial and annealed microstructure. (a) initial 2 μm , (b) 5 μm , (c) 15 μm and (d) 80 μm .

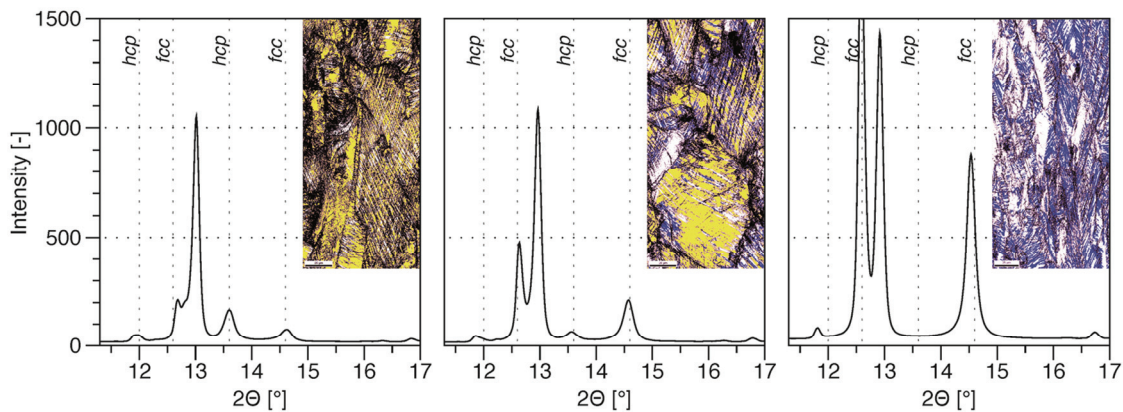


Fig. 2. Influence of temperature on active deformation mechanism for 123 K (left), 293 K (center) and 423 K (right).

5. RESULTS

Before deformation the microstructure of the investigated samples doesn't show any deformation structures and is fully austenitic. Light optical micrographs of the initial structure can be seen in figure 1. With increasing annealing temperature the initial banding structure is disappearing and the grain size is raised significantly. The calculated stacking fault energy, XRD and EBSD results lead to the conclusion, that twinning is favored at in-

quired for a nucleus of ε -martensite as reported by Olson and Cohen (1974). By increasing the grain size, the probability of finding a nucleation site for ε -martensite is improved according to Jiang et al. (1995). The increasement of the martensite start temperature with a raised grain size, was also described by Yang and Bhadeshia (2009), can affect the creation of ε -martensite. The simulation results were obtained by RVEs with a total number of 500 grains, which were generated for each microstructure and testing temperature. The hardening of each grain within the RVE is mainly depended on the



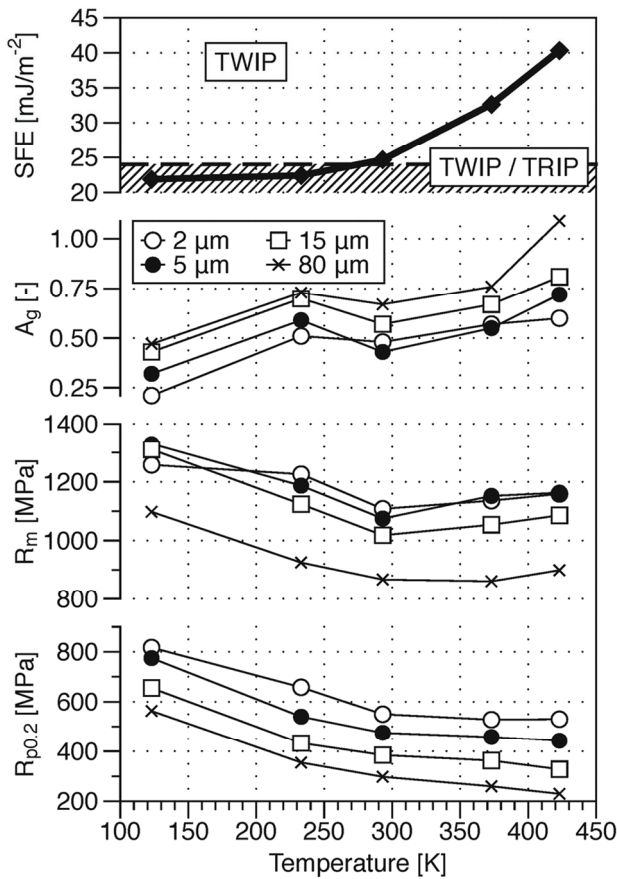


Fig. 3. Experimental results of mechanical properties and calculated stacking fault energy for a testing temperature range from 123 K to 423 K and for different microstructures with 2 μm, 5 μm, 15 μm and 80 μm.

local chemical composition on the SFE was incorporated in the model. The orientation is also respected and determined for each grain by varying the Taylor factor. By a locally defined SFE and Taylor factor within the RVE, the critical twinning stress was calculated locally according to equation 5. The distribution of manganese is assumed according to the EDX measurements, which were done on samples with the same microstructure as the RVE. The experimental and calculated homogenized hardening flow curves are shown in figure 4. By identifying the parameters f_{sat} and for equations 6 and 9, the accuracy of the calculated curves match the experimental results well for all temperatures and grain sizes. The active deformation mechanism and phase fractions of twins and ϵ -martensite are plotted in figure 5. The influence of temperature on twinning and phase transformation is in good accordance with EBSD results in figure 2. At room temperature phase transformation and twinning is active and contribute to the overall hardening. With increased temperature, only twinning is present, where ϵ -martensite formation is prevailing for a temperature of 123 K (figure 5).

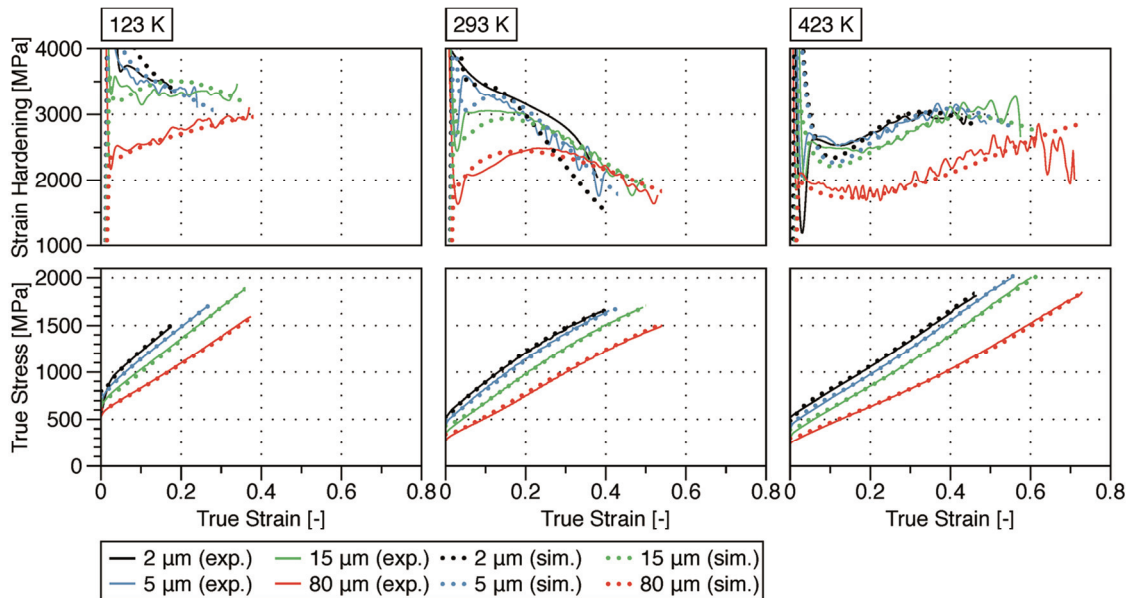


Fig. 4. Experimental and calculated flow- and hardening curves for 123 K, 293 K and 423 K and for different microstructures with 2 μm, 5 μm, 15 μm and 80 μm.

dominating deformation mechanism. By assuming a statistical distribution within the banded microstructure of manganese and carbon, the effect of the



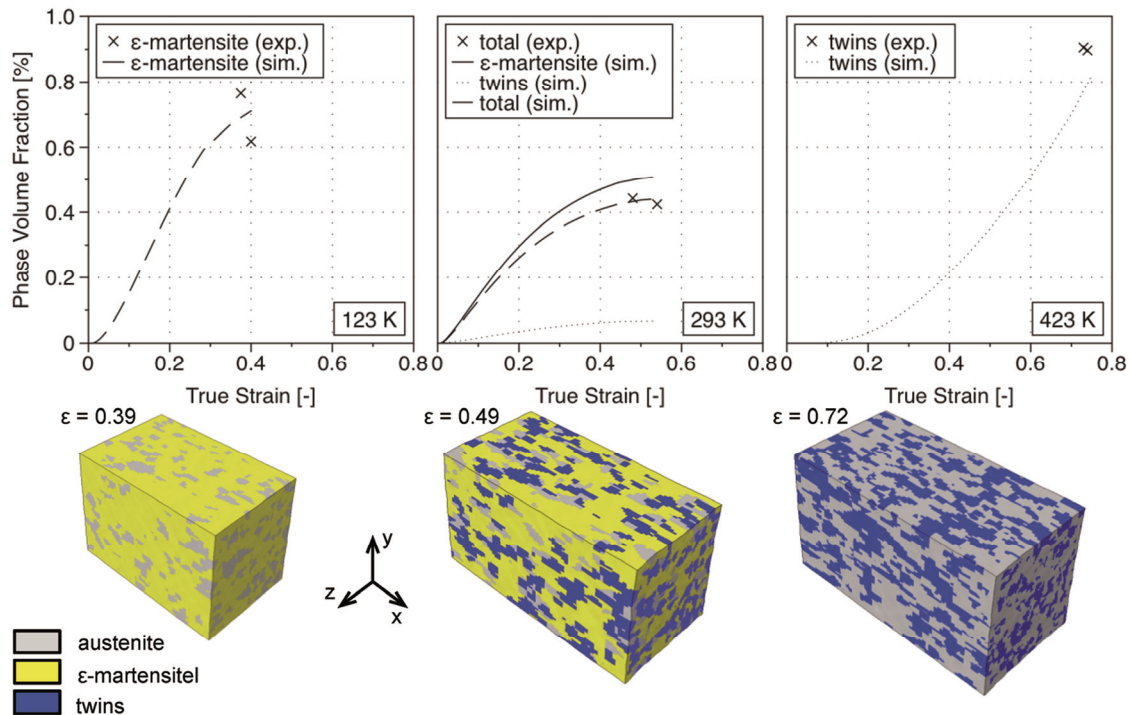


Fig. 5. Experimental and calculated phase fractions for twins and ϵ -martensite for 123 K, 293 K and 423 K for a grain size of 80 μm .]

6. CONCLUSION

The distribution of manganese and carbon have an effect on the SFE and consequently on the active deformation mechanism. Furthermore the microstructure also affects the dominating deformation mechanism at low SFE's by altering the probability of ϵ -martensite nucleation. These factors were successfully implemented in the RVE model, combined with a proper representation of the microstructure and Taylor factor distribution. By calculating the hardening behavior for each grain, multiple active deformation mechanism can be included. The model is valid for the investigated temperature and grain size range and matches the experimental results well. Nevertheless it is not possible to account for the grain rotation and local temperature increase. The change of the Taylor factor has a major impact on the critical twinning stress. The local temperature change additionally alters the SFE and consequently the active deformation mechanism.

ACKNOWLEDGEMENTS

The SFB 761 is gratefully acknowledged for the material supply and the financial support.

REFERENCES

- Allain, S., Chateau, J., Bouaziz, O., 2004a, A physical model of the twinning-induced plasticity effect in a high manganese austenitic steel, *Materials Science and Engineering A-Structural Materials Properties Microstructure and Processing*, 387, 143-147.
- Allain, S., Chateau, J.P., Bouaziz, O., Migot, S., Guelton, N., 2004b, Correlations between the calculated stacking fault energy and the plasticity mechanisms in FeMnC alloys, *Materials Science and Engineering: A*, 387-389, 158-162.
- Allain, S., Chateau, J.P., Dahmoun, D., Bouaziz, O., 2004c, Modeling of mechanical twinning in a high manganese content austenitic steel, *Materials Science and Engineering: A*, 387-389, 272-276.
- Bouaziz, O., Allain, S., Scott, C., 2008, Effect of grain and twin boundaries on the hardening mechanisms of twinning-induced plasticity steels, *Scripta Materialia*, 58, 484-487.
- Bouquerel, J., Verbeke, K., DeCooman, B., 2006, Microstructure-based model for the static mechanical behaviour of multiphase steels, *Acta Materialia*, 54, 1443-1456.
- Choi, H.C., Ha, T.K., Shin, H.C., Chang, Y.W., 1999, The formation kinetics of deformation twin and deformation induced epsilon-martensite in an austenitic Fe-C-Mn steel, *Scripta Materialia*, 40, 1171-1177.
- Dumay, A., Chateau, J.P., Allain, S., Migot, S., Bouaziz, O., 2008, Influence of addition elements on the stacking-fault energy and mechanical properties of an austenitic Fe-Mn-C steel, *Materials Science and Engineering: A*, 483-484, 184-187.
- Frommeyer, G., Brück, U., Neumann, P., 2003, Supra-ductile and high strength manganese-trip and twip steels for high energy absorption purposes, *ISIJ International*, 43, 438-446.
- Geuzaine, C., Remacle, J.F., 2009, Gmsh: A 3-d finite element mesh generator with built-in pre- and post-processing



- facilities, *International Journal for Numerical Methods in Engineering*, 79, 1309-1331.
- Gutierrez-Urrutia, I., Zaefferer, S., Raabe, D., 2010, The effect of grain size and grain orientation on deformation twinning in a Fe-22 wt.% Mn-0.6 wt.% C TWIP steel, *Materials Science and Engineering A-Structural Materials Properties Microstructure and Processing*, 527, 3552-3560.
- Jiang, B., Sun, L., Li, R., Hsu, T., 1995, Influence of austenite grain size on γ - ϵ martensitic transformation temperature in Fe-Mn-Si-Cr alloys, *Scripta Metallurgica et Materialia*, 33, 63-68.
- Jin, J.E., Lee, Y.K., 2009, Strain hardening behavior of a Fe₁₈Mn_{0.6}C_{1.5}Al TWIP steel, *Materials Science and Engineering: A*, 527, 157-161.
- Kassem, G.A., 2009, *Micromechanical Material Models for Polymer Composites Through Advanced Numerical Simulation Techniques*, Ph.D. thesis, RWTH Aachen.
- Kocks, U., Mecking, H., 2003, Physics and phenomenology of strain hardening: the fcc case, *Progress in Materials Science*, 48, 171-273.
- Lee, Y.K., Choi, C., 2000, Driving force for ϵ -martensitic transformation and stacking fault energy of ϵ in Fe-Mn binary system, *Metallurgical and Materials Transactions A*, 31, 355-360.
- Melchior, M., 2009, *Modelling of texture and hardening of TWIP steel*, Ph.D. thesis, Universite catholique de Louvain.
- Olson, G.B., Cohen, M., 1974, Kinetics of strain-induced martensitic nucleation, *Metallurgical and Materials Transactions A*, 6A, 791-795.
- Rycroft, C.H., 2009, Voro++: A three-dimensional voronoi cell library in c++, *Chaos: An Interdisciplinary Journal of Nonlinear Science*, 19.
- Saeed-Akbari, A., Imlau, J., Prahl, U., Bleck, W., 2009, Derivation and variation in composition-dependent stacking fault energy maps based on subregular solution model in high-manganese steels, *Metallurgical and Materials Transactions A*, 40A, 3076-3090.
- Saeed-Akbari, A., Mosecker, L., Schwedt, A., Bleck, W., 2011, Characterization and prediction of flow behavior in high-manganese twinning induced plasticity steels: Part 1. mechanism maps and work-hardening behavior, *Metallurgical and Materials Transactions A*, 43A, 1688-1704.
- Saeed-Akbari, A., Schwedt, A., Bleck, W., 2012, Low stacking fault energy steels in the context of manganese-rich iron-based alloys, *Scripta Materialia*, 66 (12), 1024-1029.
- Yang, H.S., Bhadeshia, H., 2009, Austenite grain size and the martensite-start temperature, *Scripta Materialia*, 60, 493-495.

UWZGLĘDNIENIE MIKROSTRUKTURY W MODELOWANIU KRZYWYCH PŁYNIĘCIA WYSOKO-MANGANOWYCH STALI Z EFEKTEM TWIP I TRIP

Streszczenie

W pracy zaproponowano model krzywych płynięcia stali z efektem TWIP i TRIP, wykorzystujący ideę reprezentatywnego elementu objętości (ang. representative volume element – RVE). Strukturę polikryształu wygenerowano poprzez dyskretyzację przestrzeni z zastosowaniem wieloboków Voronoi. Do opisu umocnienia materiału wykorzystano model wykorzystujący ewolucję populacji dyslokacji, bliźniakowanie oraz gęstość martenzytu epsilon. Odształcenie plastyczne analizowano numerycznie stosując okresowe warunki brzegowe w RVE. Oprócz uwzględnienia wpływu temperatury i prędkości odształcenia rozważono też wpływ nierównomierności składu chemicznego. Weryfikację doświadczalną modelu przeprowadzono dla próby jednoosiowego rozciągania próbek płaskich.

Received: June 28, 2012

Received in a revised form: October 16, 2012

Accepted: November 19, 2012

